www.rericjournal.ait.ac.th

Optimum Turbine and Compressor Inlet Pressures for Maximum Net Specific Work of a Regenerative Supercritical Carbon Dioxide Brayton Cycle

Sompop Jarungthammachote* and Kitipong Jaojaruek^, [1]

ARTICLE INFO

Article history:
Received 23 February 2025
Received in revised form
27 April 2025
Accepted 15 May 2025

Keywords:
Maximum net specific work
Optimum pressure
Real gas properties
Supercritical CO_2 Brayton cycle

ABSTRACT

The Supercritical CO_2 (sCO_2) Brayton cycle has recently gained more attention and is considered a promising power cycle. In this study, relationships for determining the optimum compressor and turbine inlet pressures, maximizing the net specific work of regenerative and simple sCO_2 Brayton cycles, were developed. A key innovation of this work lies in expressing these relationships in terms of dimensionless quantities which have not been previously reported in the literature. The effects of turbine and compressor inlet pressures, inlet temperatures as well as their efficiencies on the optimum compressor and turbine inlet pressures and the maximum net specific work were investigated. The results indicated that, under some operating conditions, no compressor inlet pressure caused a peak of net specific work and the criterion of the optimum compressor inlet pressure could not be satisfied. An increase in turbine inlet pressure led to a slight reduction in the optimum compressor inlet pressure, while an increase in compressor inlet pressure resulted in an increase in the optimum turbine inlet pressure. Both increases had positive effects on the maximum net specific work. The optimum turbine inlet pressure increased with an increase in turbine inlet temperature and decreased with an increase in compressor inlet temperature. However, increases in both temperatures caused opposite changes in the optimum compressor inlet pressure. Increases in compressor and turbine efficiencies resulted in reducing the optimum compressor and increasing the optimum turbine inlet pressures. The optimum pressure calculated based on the ideal gas assumption is not applicable for sCO_2 Brayton cycle, as it could result in an absolute percentage difference of 113.01% in the prediction of the optimum compressor inlet pressure

1. INTRODUCTION

The supercritical carbon dioxide (sCO_2) Brayton cycle is a high efficiency cycle as it requires less compression work close to the critical point [1]. Research works involving its applications for nuclear power generation and concentrated solar thermal power have revealed its potential for high efficiency [2]-[5]. The sCO_2 Brayton cycle offers several distinct advantages over traditional power generation cycles, such as Rankine cycles. Its superior thermodynamic efficiency and ability to operate at high pressures with compact equipment make it a promising choice, especially when integrated with renewable energy systems [6][7]. Moreover, sCO_2 is a nontoxic and nonflammable substance, therefore, it may not cause serious damage when it is accidentally released.

Various cycle layouts, including regenerative, recompression, partial cooling, and intercooling cycles, have been investigated for their performances [8][9]. The regenerative Brayton cycle is a modified simple Brayton cycle to enhance thermal efficiency. It has a single regenerator recovering heat from the turbine's exhaust and supplying recovered heat to CO_2 before entering the heater. Its simplicity is an advantage. However, its configuration can be modified to gain more efficiency. The recompression cycle uses an additional compressor to increase the pressure of CO_2, which is split after flowing out of a low temperature recuperator. Even though the recompression cycle can improve thermal efficiency, the complexity of recompression cycles can result in higher capital costs and maintenance requirements [10]. Each layout has unique benefits making it crucial to select the appropriate configuration based on specific application requirements.

There are two important operating points of power cycles, like Brayton cycle, the maximum efficiency and the maximum net work output operating points. [11] pointed out that the operational regime of Brayton cycles should be between the optimum regimes by maximizing the net work output and maximizing thermal efficiency. However, if the net work output from the Brayton cycle is mainly required, the operating condition must shift to the optimum point maximizing

*Department of Mechanical Engineering, Faculty of Engineering at Sriracha,Kasetsart University Si Racha Campus, 199 Sukhumvit Road, Chonburi, 20230, Thailand.

^Department of Mechanical Engineering, Faculty of Engineering KPS, Kasetsart University Kamphaeng Saen Campus, Nakhon Pathom, 73140, Thailand.

1 Corresponding author;
Tel: 66813742507, Fax: + 6634355310.
E-mail: fengkpj@ku.ac.th

net work output. [11] investigated optimum pressure ratios maximizing the 1st and 2nd law efficiencies and work output of the ideal open regenerative Brayton cycle. The analysis was done based on the ideal gas assumption and the analysis result showed that the optimum pressure ratio maximizing the 1st law efficiency was less than the optimum pressure ratio maximizing the work output for the regenerator effectiveness greater than 0.7. Moreover, the regenerator effectiveness did not affect the optimum pressure ratio for maximum work output analyzed based on the ideal gas working fluid. [12] studied the turbine inlet state in a transcritical CO_2 cycle with an internal heat exchanger that could maximize the efficiency and net specific work output rate. [13] proposed a solar driven transcritical CO_2 power cycle and effects of turbine inlet pressure and temperature on the net power output were investigated. Their result showed that there is an existence of an optimum turbine inlet pressure corresponding to maximum net power output. A sCO_2 Brayton cycle with multi-stage compression and intercooling was investigated by [14]. The effects of the lowest cycle pressure and intermedia pressure on the maximum specific work and the 2nd efficiency were observed. An optimum combination of lowest cycle pressure and intermediate pressure exists for which specific work output or 2nd law efficiency of the two-stage compression and intercooling sCO_2 cycle was maximized. [15] performed optimization of simple and regenerative Brayton cycles using air as working fluid. From their result, the net power output was at its maximum in both cycles at the lowest compressor inlet temperature (288 K). At fixed turbine inlet temperature and pressure ratio used in their study, the net power output linearly decreased as compressor inlet temperature increases. Therefore, no global maximum net power output was found between minimum and maximum compressor inlet temperatures. Thermal efficiency and net specific power output of simple and regenerative Brayton cycles were analyzed for nine working fluids [16]. The analysis showed that real gases produce lower net specific work output for the same heat input compared to the perfect gases. Moreover, sCO_2 had the highest thermal efficiency of all analyzed working fluids because, in the operation zone defined in the study, the liquid-like behavior of sCO_2 resulted in a significant decrease in the specific compressor work leading to the higher net specific work output and higher thermal efficiency. Ehsan *et al.* [17] presented a comparative analysis of direct and indirect dry cooling systems designed for a 25 MW sCO_2-based CSP plant. The work notably utilized a one-dimensional nodal MATLAB model that captures the nonlinear variation of sCO_2 properties near the critical point, ensuring accurate prediction of heat transfer and pressure drop characteristics. In a more comprehensive follow-up study, Ehsan *et al.* [18] extended this analysis by evaluating the performance of two advanced sCO_2 Brayton cycle configurations, recompression and partial cooling, each integrated with a natural draft dry cooling tower (NDDCT). Their results demonstrated that recompression cycles exhibit superior thermal efficiency at lower compressor inlet temperatures (30-49 °C). Furthermore, the research emphasized that proper design and optimization of the NDDCT significantly impacts cycle efficiency and the required size of the solar field, thereby influencing the overall economic viability of CSP systems. The optimization of sCO_2 recuperated and recompression configurations of sCO_2 Brayton cycles was carried out using genetic algorithm (GA) [19]. The main objective function is the net cycle power output in order to account for the maximum extracted heat out of a hot exhaust stream. The use of GA in optimization of sCO_2 Brayton cycles to maximize the power output was found again in the works of [20] and [21]. For complicated optimization problems in supercritical Brayton cycles, special optimization algorithms and techniques were required [22]-[24].

Based on the literature review mentioned above, if the real gas properties are considered, special optimization techniques are applied for complicated optimization problems. However, a simple search technique (or iteration calculation) was frequently used in many studies. The optimum operating parameters, such as turbine inlet pressure (or pressure ratio), were found based on the iterative calculation in which the net work outputs or the thermal efficiencies were tested at different values of the parameter. The value of the parameter given the maximum net work output or thermal efficiency was found to be the optimum value. Therefore, if an increment of the parameter is not small enough, this approach may give the same optimum values of the parameter at two different conditions and this can be questionable. Another issue found is that the ideal gas assumption has been often applied to find the optimum turbine inlet pressure maximizing the thermal efficiency or maximizing the net work output, such as found in [25], [26]. In practice, the real gas behavior is different from the ideal gas one, especially at high pressure like in supercritical region. Therefore, the ideal gas model may not give an accurate result for high pressure applications, like in the supercritical Brayton cycle.

In this study, a single equation used to determine the optimum turbine inlet pressure maximizing the net specific work of regenerative sCO_2 Brayton cycle was developed. The equation is expressed in terms of dimensionless quantities derived from real gas properties, including temperatures, densities, and the thermal expansion coefficient. Similarly, another equation to find the optimum compressor inlet pressure, following a structure analogous to the first equation, was also developed. These equations are, in fact, applicable not only to CO_2, but also to other gases employed as working fluids in regenerative Brayton cycles. To the best of the author's knowledge, no such equations have been proposed in the literature. The remainder of the paper is structured as follows. In section 2, a description of the regenerative sCO_2 Brayton cycle is presented. Section 3 depicts the development of mathematical models for the optimum turbine and compressor inlet pressures maximizing the net specific work and thermal efficiency. Model validation is also presented in this section. The effects of operating parameters, such as

compressor and turbine inlet temperatures, on the optimum pressures are discussed in sections 4. Finally, conclusions are drawn in Section 5.

The outcomes of this study, particularly the dimensionless correlations for determining optimum inlet pressures, are relevant the optimization of sCO_2-based power systems for industrial applications. These include waste heat recovery from gas turbines and concentrated solar power (CSP) plants where the power output from the cycle is primary concern. The proposed equations can serve as a first-level design tool to guide pressure selection before conducting more detailed simulations or experiments. Furthermore, the high net specific work obtained under optimal conditions can contribute to reducing the overall size and cost of turbomachinery, making sCO_2 cycles increasingly viable for small-to-medium scale energy systems.

2. CYCLES DESCRIPTION

In this study, the regenerative sCO_2 Brayton cycle is investigated and its schematic is presented in Figure 1. Numbers shown in Figure 1 indicate the thermodynamic states in the cycle.

The net specific work of the regenerative Brayton cycle can be calculated from

$$w_{net} = w_T - w_C = (h_3 - h_{4s})\eta_T - \frac{(h_{2s} - h_1)}{\eta_C} \quad (1)$$

In this study, η_T and η_C are assumed to be constant.

3. MODEL DEVELOPMENT

3.1 Optimum Turbine Inlet Pressure

To find the optimum turbine inlet pressure, P_{3opt}, that maximizes the net specific work, the first derivative of the net specific work with respect to P_3 is found and set to be zero, as expressed in Equation 2.

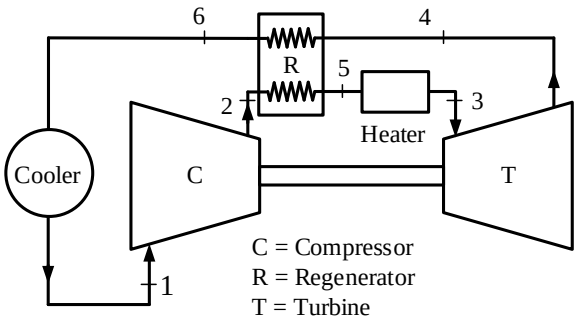

Fig. 1. Schematic of a regenerative sCO_2 Brayton cycle.

$$\frac{\partial w_{net}}{\partial P_3} = \eta_T \frac{\partial}{\partial P_3}(h_3 - h_{4s}) - \frac{1}{\eta_C}\frac{\partial}{\partial P_3}(h_{2s} - h_1) = 0 \quad (2)$$

Based on the Maxwell relationship and a fixed turbine inlet temperature T_3, the derivative on the right-hand side of Equation 2 can be transformed to [27].

$$\frac{\partial w_{net}}{\partial P_3} = \eta_T \left(T_3 \left(\frac{\partial s_3}{\partial P_3}\right)_{T_3} + \frac{1}{\rho_3} \right) - \eta_T T_{4s} \left(\frac{\partial s_3}{\partial P_3}\right)_{T_3} - \frac{1}{\eta_C \rho_{2s}} = 0 \quad (3a)$$

$$\eta_T \left(\frac{\partial s_3}{\partial P_3}\right)_{T_3} (T_3 - T_{4s}) + \frac{\eta_T}{\rho_3} - \frac{1}{\eta_C \rho_{2s}} = 0 \quad (3b)$$

The term $(\partial s/\partial P)_T$ can be replaced by $-(\partial v/\partial T)_P$ and it relates to a fluid property called the thermal expansion coefficient (or the thermal expansivity), β, which is defined as

$$\beta = \frac{1}{v}\left(\frac{\partial v}{\partial T}\right)_P = -\frac{1}{\rho}\left(\frac{\partial \rho}{\partial T}\right)_P \quad (4)$$

Therefore, Equation 3b can be written as:

$$\eta_T \left(-\frac{\beta_3}{\rho_3}\right)_{T_3} (T_3 - T_{4s}) + \frac{\eta_T}{\rho_3} - \frac{1}{\eta_C \rho_{2s}} = 0 \quad (5)$$

Multiplying Equation 5 with $-\frac{\rho_3}{\eta_T}$ gives the following equation in which each term is a dimensionless quantity.

$$f_1 = \beta_3(T_3 - T_{4s}) + \frac{\rho_3}{\rho_{2s}}\frac{1}{\eta_C \eta_T} - 1 = 0 \quad (6)$$

If the working fluid is assumed to be an ideal gas, the thermal expansion coefficient in Equation 6 becomes$\beta_3 = 1/T_3$. Applying the ideal gas law, $P = \rho RT$, and the isentropic relation to processes 3-4s and 1-2s, these surprisingly lead to:

$$\left(\frac{P_{3opt,IG}}{P_1}\right) = \left(\frac{T_3}{T_1}\eta_T \eta_C\right)^{k/2(k-1)} \quad (7)$$

The optimum pressure ratio for the ideal gas working fluid as shown in Equation 7 can often be found in literature, such as Gülen's book [26] and Javanshir *et al.*'s work [16] in which the optimum pressure ratio was obtained from the derivative of the ideal gas specific work output of the cycle. However, the way to find the optimum turbine inlet pressure using real gas properties as expressed in Equation 6, as author knowledge, has not been found in literature. Moreover, Equation 6, in fact, can be applied not only to CO_2 gas but also to other gases.

3.2 Optimum Compressor Inlet Pressure

The turbine inlet pressure strongly affects the net specific work of the cycle. To reach a very high turbine inlet pressure, the compressor outlet pressure is limited due to technological constraints [19][28][29] have mentioned that the upper limit of compressor pressure is caused by the structural capability of heat exchangers. In their study, the compressor outlet pressure was limited to 33 MPa. Therefore, the second optimization model in this study is developed to find the optimum compressor inlet pressure, P_{1opt}, which causes the maximum net specific work, from a known turbine inlet state, (P_3, T_3), and compressor inlet temperature T_1.

The first derivative of the net specific work with respect to P_1 is set to equal zero.

$$\frac{\partial w_{net}}{\partial P_1} = \eta_T \frac{\partial}{\partial P_1}(h_3 - h_{4s}) - \frac{1}{\eta_C}\frac{\partial}{\partial P_1}(h_{2s} - h_1) = 0 \quad (8)$$

As P_3 and T_3 are fixed at specific values, the enthalpy at state 3 is independent of P_1 and, thus, $\partial h_3/\partial P_1 = 0$. Based on similar relationships used in the first model, Equation 8 can be transformed to:

$$\frac{\partial w_{net}}{\partial P_1} = \eta_T\left(-\frac{1}{\rho_{4s}}\right) - \frac{1}{\eta_C}T_{2s}\left(\frac{\partial s_1}{\partial P_1}\right)_{T_1} + \frac{1}{\eta_C}T_1\left(\frac{\partial s_1}{\partial P_1}\right)_{T_1} + \frac{1}{\eta_C\rho_1} = 0 \quad (9)$$

Applying Equation 4 to the term $(\partial s_1/\partial P_1)_{T_1}$ in Equation 9 and arranging equation, these finally give:

$$0 = -\frac{\eta_T}{\rho_{4s}} + \frac{1}{\rho_1\eta_C} - \frac{1}{\eta_C}(T_{2s} - T_1)\left(-\frac{\beta_1}{\rho_1}\right) \quad (10)$$

Multiplying Equation 10 with $-\rho_1\eta_C$ yields the following equation.

$$f_2 = \beta_1(T_1 - T_{2s}) + \frac{\rho_1}{\rho_{4s}}\eta_T\eta_C - 1 = 0 \quad (11)$$

Each term in Equation 11 is a dimensionless quantity and Equation 11 has similar structure as expressed in Equation 6. As the author has done literature review, no such equation for calculating the optimum compressor inlet pressure has been found.

For the ideal gas working fluid, $P_{1opt,IG}$ can be obtained in the similar way as $P_{3opt,IG}$ was found. The equation to calculate$P_{1opt,IG}$ is the same as Equation 11 which is developed to determine $P_{3opt,IG}$, but in this case, P_3 is known and $P_{1opt,IG}$ is to be determined.

To find P_{3opt} using Equation 6 or P_{1opt} using Equation 11, the calculation procedures are explained in Figures 2(a) and 2(b), respectively.

In the figures, only calculation steps with solid-line frames are required to find P_{3opt} and P_{1opt}. The calculation steps with dashed-line frames are required to calculate the net specific work and the thermal efficiency if these performance indicators are desired to be known. Due to limited space and outside the scope of this study, the calculation and discussion of thermal efficiency are neglected. Pressure drops across heat exchangers can be considered in both models. The value of pressure drops, represented by ΔP, in each calculation step may not be the same and its value can be given in terms of percentage [30] or fraction [19].

The properties of CO_2 used in this study were obtained from the multiparameter equation of state developed by [31]. The calculation of the thermodynamic properties in this equation of state requires to know the density ρ and the temperature T. Therefore, in Figures 2(a) and (2), other properties calculated from this equation of state require the values of ρ and T. The ideal gas CO_2 specific heat ratio k is 1.2885. A polynomial equation of specific heat at constant pressure was taken from McBride *et al.*'s work [32]. The value of k of ideal gas CO_2 is calculated at 298.15 K.

Before moving to the next section, it should be pointed out here that the optimum turbine inlet pressure and the optimum compressor inlet pressure obtained from solving Equation 6 and Equation 11, respectively, can also be applied to the simple sCO_2 Brayton cycle. The subscript numbers, representing thermodynamic states denote the same thermodynamic states in the regenerative and in the simple sCO_2 Brayton cycles, such as state 2 is the compressor outlet state.

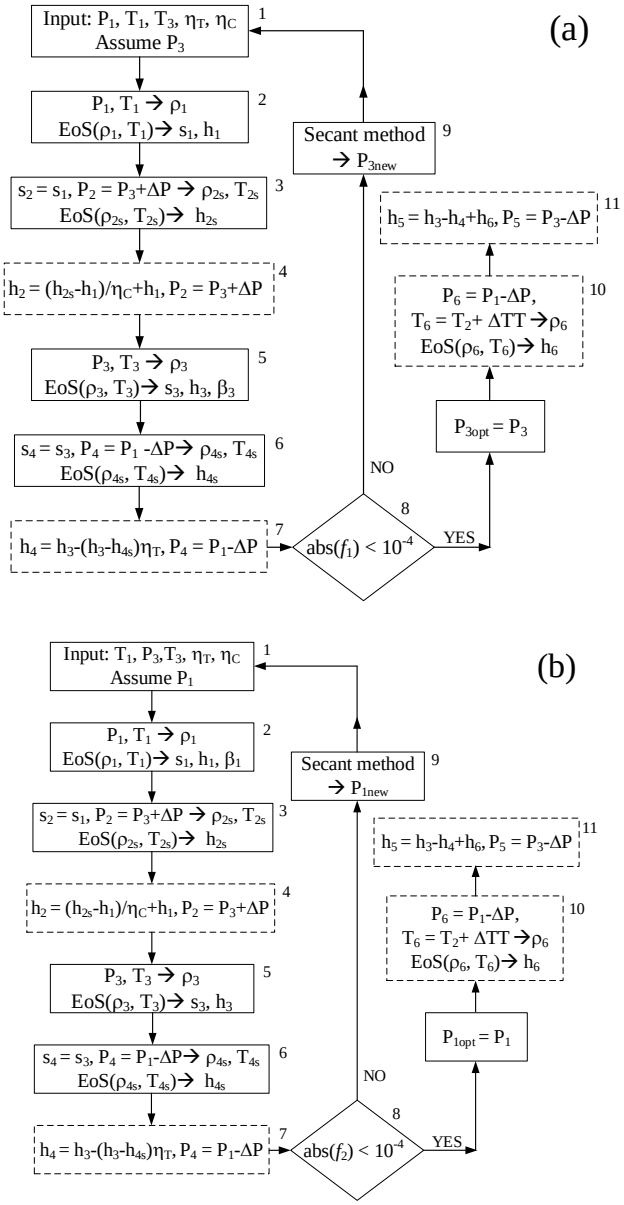

Fig. 2. Calculation procedure for (a) P_{3opt}, (b) P_{1opt}.

3.3 Model Validation

The models developed in this study require properties of CO_2, calculated from Span and Wagner's equation of state. The first validation was done to verify the properties calculation in the models. The reference values were determined by utilizing the properties of CO_2 obtained from NIST [33] at different thermodynamic states. The comparison of properties from the models and NIST shows the agreement.

To validate the optimum pressures obtained from the developed models, the validation is divided into two parts. The first validation is carried out for the optimum compressor inlet pressure. The calculation results from the work of [14] were used for comparison with the results of the developed model. The second validation is performed for the optimum turbine inlet pressure prediction. The reference results were obtained from the iterative calculation. The net specific works were calculated for small intervals of turbine inlet pressure. Then, the turbine inlet pressure maximizing net specific

work was set as the reference value of the optimum turbine inlet pressure.

Table 1 presents the comparison result of the optimum compressor inlet pressure of the regenerative sCO_2 Brayton cycle obtained from Mondal and De's work [14] and that from the developed model in this study. The comparison results of P_{1opt} show that the absolute relative difference (ARD) values are small for all comparison cases. In the work of Mondal and De, the net specific works were calculated for small intervals of pressure (0.05 MPa) to find P_{1opt}. This may be the reason that P_{1opt} of the cases that P_3 = 14 MPa and 15 MPa have the same value. However, these P_{1opt} should not be the same value for different values of P_3. Based on the model developed in this work, P_{1opt} for P_3 = 14 MPa and 15 MPa are about 8.27 MPa and 8.30 MPa, respectively. Difference values between net specific works from Mondal and De's study and that from the present work can be negligible as ARD values are very small. From ARD values in P_{1opt} and w_{net} comparisons, these indicate good agreement between the results from the developed model in this study and that from Mondal and De's work [14].

Table 1. Validation of the model for optimum compressor inlet pressure.

P_3 (MPa)	P_{10pt} (MPa)		w_{net} (kJ/kg)		ARD % (P_{10pt})	ARD % (w_{net})
	Mondal and De's work	Present work	Mondal and De's work	Present work		
12	8.20	8.198	14.09	14.08	0.03	0.075
13	8.25	8.233	16.08	16.09	0.20	0.083
14	8.30	8.268	17.64	17.65	0.38	0.078
15	8.30	8.304	18.82	18.83	0.04	0.054
16	8.35	8.340	19.67	19.68	0.12	0.060
17	8.40	8.377	20.27	20.26	0.27	0.056

The validation of model for optimum turbine inlet pressure was conducted by comparing the result of the developed model and that determined from the iterative calculation. In the validation, cycle parameters were obtained from the work of Hossain *et al.* (2021). These are P_1 = 7.5 MPa, T_1 = 305.15K, T_3 = 646.15K, η_T = 0.8, and η_C = 0.75. No pressure drop and 0.5% pressure drops across heat exchangers are considered. The iterative calculation of net specific work was done from P_3 = 15.0 MPa to 45.0 MPa with an increment of 0.075 MPa for both pressure drop cases. The optimum turbine inlet pressures from the iterative calculations were used as reference values small. From ARD values in P_{1opt} and w_{net} comparisons, these indicate good agreement between the results from the developed model in this study and that from Mondal and De's work [14].

The validation of model for optimum turbine inlet pressure was conducted by comparing the result of the developed model and that determined from the iterative calculation. In the validation, cycle parameters were obtained from the work of [34]. These are P_1 = 7.5 MPa, T_1 = 305.15K, T_3 = 646.15K, η_T = 0.8, and η_C = 0.75. No pressure drop and 0.5% pressure drops across heat exchangers are considered. The iterative calculation of net specific work was done from P_3 = 15.0 MPa to 45.0 MPa with an increment of 0.075 MPa for both pressure drop cases. The optimum turbine inlet pressures from the iterative calculations were used as reference values and employed to compare with the optimum turbine inlet pressures from the developed model. The comparison result is given in Table 2 and it indicates that, in each case of pressure drop, P_{3opt} from the developed model agrees with that from the iterative calculation.

Table 2. Validation of the model for optimum turbine inlet pressure.

Case	P_{3opt} (MPa)	
	Iterative calculation	Developed model
No pressure drop	32.894	32.893
0.5% pressure drops	33.070	33.070

Although our model demonstrates consistency with other theoretical studies, its real-world applicability requires further validation under specific conditions.

4. RESULTS AND DISCUSSION

To investigate the optimum turbine inlet pressures at different compressor inlet states and the optimum compressor inlet pressures at different turbine inlet states, the values of cycle parameters employed in calculations are summarized in Table 3. In this study the pressure drops across heat exchangers are assumed to be zero because the results of the developed models are needed to compare with the results of the ideal gas model in which the pressure drops are not considered.

Table 3. Operating parameters of the regenerative sCO_2 Brayton cycle.

Parameter	Value
Turbine inlet temperature, T_3	646.15 K
Compressor inlet temperature, T_1	308.15 K
Isentropic efficiency of turbine, η_T	0.8
Isentropic efficiency of compressor, η_C	0.75
Pressure drops across heat exchangers	0.0%

4.1 Optimum Turbine Inlet Pressure

Figure 3 shows the effect of P_1 on P_{3opt} when other parameters are fixed the values as defined in Table 3. The figure presents that P_{3opt} increases with increasing P_1. The changing of P_{3opt} can be divided into three intervals. At the beginning of changing P_1 from 7.5 to 7.8 MPa, P_{3opt} increases from 28.22 MPa to 31.28 MPa. Beyond this point, when P_1 increases, P_{3opt} sharply increases. After P_1 reaches 8.2 MPa, increasing rate of P_{3opt} reduces.

$w_{net,max}$ related to P_{3opt} is also presented in Figure 3. It indicates that the shape of $w_{net,max}$ quite similar to the shape of P_{3opt}. When P_{3opt} changes with high increasing rate, $w_{net,max}$ also strongly increases. However, until P_1 approaches to 8.6 MPa, associated with P_{3opt} about 41.13 MPa, $w_{net,max}$ reaches the maximum point that is 68.27 kJ/kg. Then, $w_{net,max}$ starts to decrease when P_1 increases.

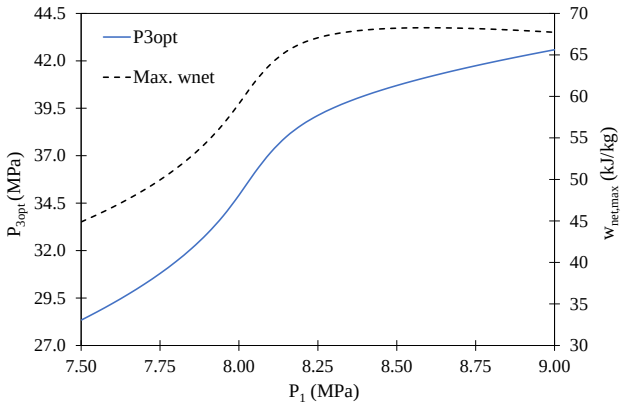

Fig. 3. Optimum turbine inlet pressure and maximum net specific work.

Table 4 shows the comparison between $P_{3opt,IG}$ obtained from the ideal gas model and P_{3opt} obtained from the model developed in this study and it expresses that the values of $P_{3opt,IG}$ are extremely lower than that of P_{3opt}. The ratio of P_{3opt} to $P_{3opt,IG}$ for all cases varies between 2.26 to 2.87. The ARD values of the comparison data are very high and vary between 55.80 and 65.12%.

Table 4. Comparison of optimum turbine inlet pressure from the ideal gas model and the developed model in this study.

P_1 (MPa)	$P_{3opt,IG}$ (MPa)	P_{3opt} (MPa)	ARD (%)
7.5	12.524	28.334	55.80
8.0	13.359	34.917	61.74
8.5	14.194	40.698	65.12
9.0	15.029	42.583	64.71

4.2 Optimum Compressor Inlet Pressure

Before the calculation result of the optimum compressor inlet pressure is presented and discussed, there is an interesting issue found during investigation of the optimum compressor inlet pressure calculation. It is that at a certain value of P_3, when T_1 or T_3 increase, there is no peak of net specific work and no zero value of f_2 found in the calculation. However, at that operating condition, if η_T or η_C reduce, the peak of net specific work may be found. For example, at operating parameters defined in Table 3 and P_3 = 13.0 MPa, the peak point of net specific work, that is maximum net specific work, is found at P_{1opt}= 8.159 MPa. However, when T_1 increases to 318.15 K, there is no peak of net specific work and the function f_2 does not cross a zero value as illustrated in Figures 4(a) and 4(b), respectively. The net specific work continuously reduces and f_2 continuously increases with positive value. At this operating condition, if T_1 = 318.15K but η_T reduces to 0.7, the maximum net specific work is found at P_{1opt}= 8.505 MPa. Therefore, the boundaries of T_1, P_3, T_3, η_T and η_C having the peak point of net specific work are difficult to define as it depends on the combinations of these 5 parameters.

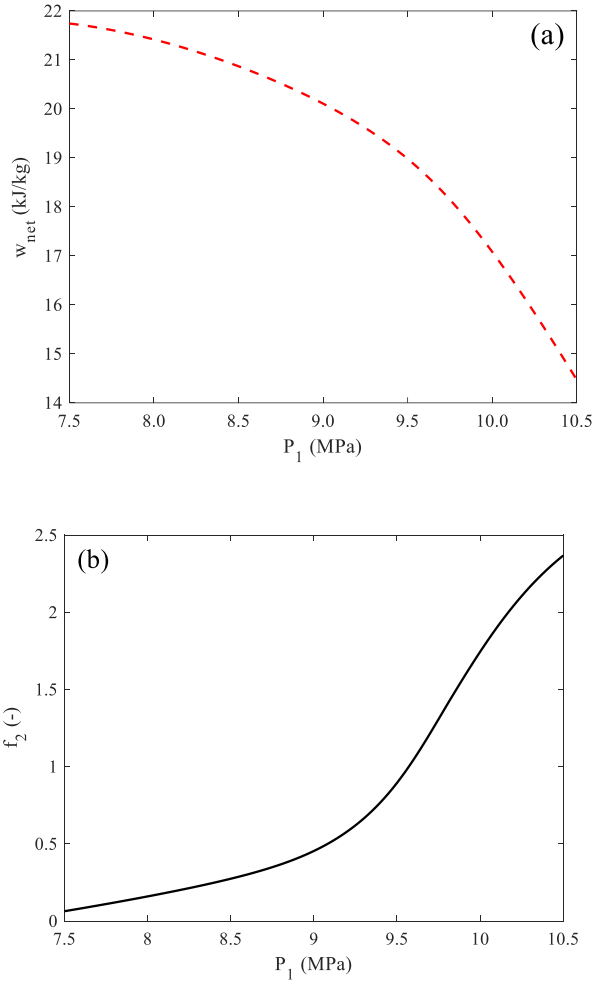

Fig. 4. (a) No peak of net specific work and (b) no zero value of f_2 for T_1 = 318.15 K, P_3 = 13 MPa, T_3 = 646.15 K, η_C = 0.75, and η_T = 0.8.

Figure 5 shows the effect of P_3 on P_{1opt} and $w_{net,max}$. From The association between P_3 and P_{1opt} can be characterized by a linear relationship. As P_3 increases from 12.0 to 33.0 MPa, there is a corresponding increase in P_{1opt} from 8.13 to 8.48 MPa. Although the variation in P_{1opt} is comparatively modest

in relation to the range of changes in P_3, the corresponding increase in $w_{net,max}$ exceeds twice as P_3 expands from 12.0 to 33.0 MPa. An interesting observation emerges from the analysis of Figures 3 and 5. The model developed to determine the optimum turbine inlet pressure, based on the operating parameters outlined in Table 3, yields P_{3opt} = 30.2 MPa associated with P_1 = 7.70 MPa (refer to Figure 3). However, it is noteworthy that this model cannot be used to identify the optimum compressor inlet pressure, as the assertion that, at identical operating parameters defined in Table 3 and P_3 = 30.2 MPa, P_{1opt} is 7.70 MPa. is not supported. As depicted in Figure 5, the optimal compressor inlet pressure for P_3 = 30.2 MPa is P_{1opt} = 8.44 MPa. Furthermore, the maximum net specific works for these cases are also different. Specifically, P_{1opt}= 8.44 MPa, corresponding to P_3 = 30.2 MPa, yields $w_{net,max}$ =65.43 kJ/kg, whereas P_{3opt} = 30.2 MPa, associated with P_1 = 7.70 MPa, results in $w_{net,max}$ = 48.75 kJ/kg.

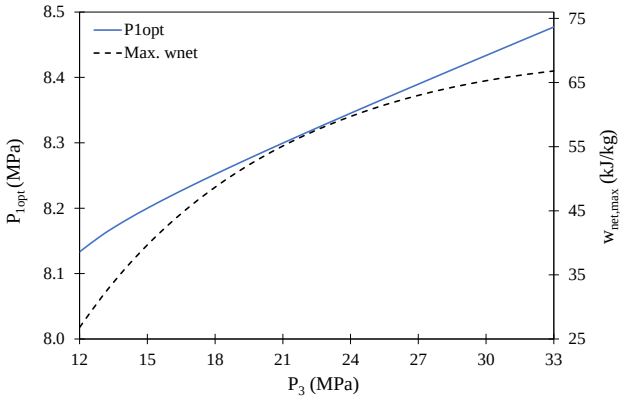

Fig. 5. Optimum compressor inlet pressure and maximum net specific work.

From Figure 5, it can be observed that when P_3 increases, the value of $w_{net,max}$ increases with varying rate. $w_{net,max}$ seems to reach a maximum at any point that P_3 is higher than 33.0 MPa. The calculation was conducted for an extended range of P_3 and the calculation result is shown in Figure 6.

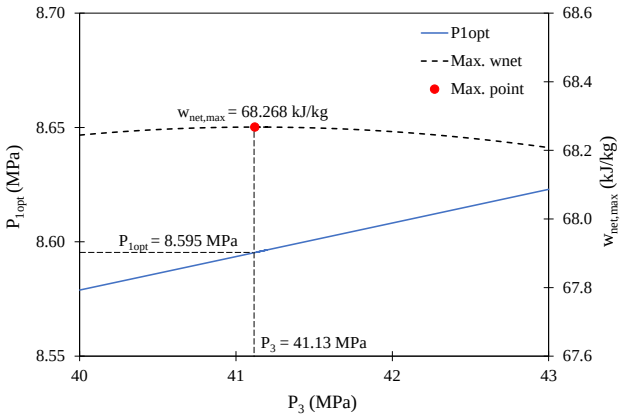

Fig. 6. Location of the maximum of $w_{net,max}$.

It expresses that the maximum of $w_{net,max}$ takes place at P_3 = 41.13 MPa and P_{1opt} = 8.595 MPa and at this point the maximum $w_{net,max}$ = 68.268 kJ/kg. It is quite interesting that at P_1 = 8.595 MPa, the developed model for P_{3opt} gives P_{3opt} = 41.13 MPa and $w_{net,max}$ = 68.268 kJ/kg (see Figure 3). It can be implied that at specific parameters defined in Table 3, the regenerative sCO_2 Brayton cycle operated at P_1 = 8.595 MPa and P_3 = 41.13 MPa gives the best net specific work output from the cycle. However, this value of P_3 may be beyond the operating pressure limitation of some types of heat exchanger.

Table 5 shows the comparison of the optimum compressor inlet pressure obtained from the ideal gas model and that from the model developed in this study. It indicates that $P_{1opt,IG}$ linearly increases when P_3 increases. This is because for fixed operating parameters, the right-hand side of Equation 7 is a constant. Therefore, the change in $P_{1opt,IG}$ is dependent on the turbine inlet pressure. Compared to P_{1opt}, its value slightly increases when the turbine inlet pressure increases. The comparison, therefore, shows a large value of ARD for the case that P_3 = 30.0 MPa. It can be implied that the ideal gas model is not suitable for estimation of the optimum compressor inlet pressure in the regenerative sCO_2 Brayton cycle.

Table 5. Comparison of optimum compressor inlet pressure from the ideal gas model and the developed model in this study.

P_3 (MPa)	$P_{1opt,IG}$ (MPa)	P_{1opt} (MPa)	ARD (%)
12.0	7.186	8.133	11.64
18.0	10.779	8.252	30.62
24.0	14.372	8.345	72.22
30.0	17.965	8.434	113.01

4.3 Effects of Compressor and Turbine Inlet Temperatures

The compressor inlet pressure was fixed at 7.5 MPa and the values of other parameters defined in Table 3 were also used. The variation of optimum turbine inlet pressures and maximum net specific works with the compressor inlet temperatures are shown in Figure 7(a). In Figure 7(b), the turbine inlet pressure was fixed at 30.0 MPa and the compressor inlet temperature was varied from 305.15 to 318.15 K to investigate its effect on the optimum compressor inlet pressure as well as the maximum net specific work. To reach the maximum net specific work at a specific value of P_1, the increase in T_1 causes decreasing P_{3opt}. However, a fixed value of turbine inlet pressure, increasing T_1 results in linearly increase in P_{1opt}. From both figures, the increase in T_1 has negative effect on $w_{net,max}$. This can be explained through the effect of temperature on fluid density and specific volume at the compressor inlet. At higher T_1, the CO_2 density decreases, resulting in an increase in specific volume. Since the compression work is proportional to the pressure change and specific volume, this leads to a higher specific compressor work. For fixed P_1, the specific compressor work slightly increases, and the specific turbine work clearly decreases when T_1 increases from 305.15 to 318.15 K. These are due to increasing T_1 results in more work

required by the compressor. But $P_{3,opt}$ decreases as T_1 increases, so the work required by the compressor to reach $P_{3,opt}$ slightly increases. As $P_{3,opt}$ decreases when T_1 increases, the specific work produced from the turbine decreases. The small increase in specific compressor work and the decrease in turbine specific work resulted in decreasing $w_{net,max}$ from 56.8 to 29.2 kJ/kg. For fixed P_3, when T_1 increases from 305.15 to 318.15 K, the compressor requires more compression work. However, since P_3 is fixed and P_{1opt} increases as T_1 increases, it causes the compressor to require less specific work. These two opposite effects on the specific work required by the compressor consequently result in a slight change of the specific compressor work. As P_3 is fixed and P_{1opt} increases as T_1 increases, the specific turbine work decreases. $w_{net,max}$, then, decreases from 70.89 to 50.46 kJ/kg.

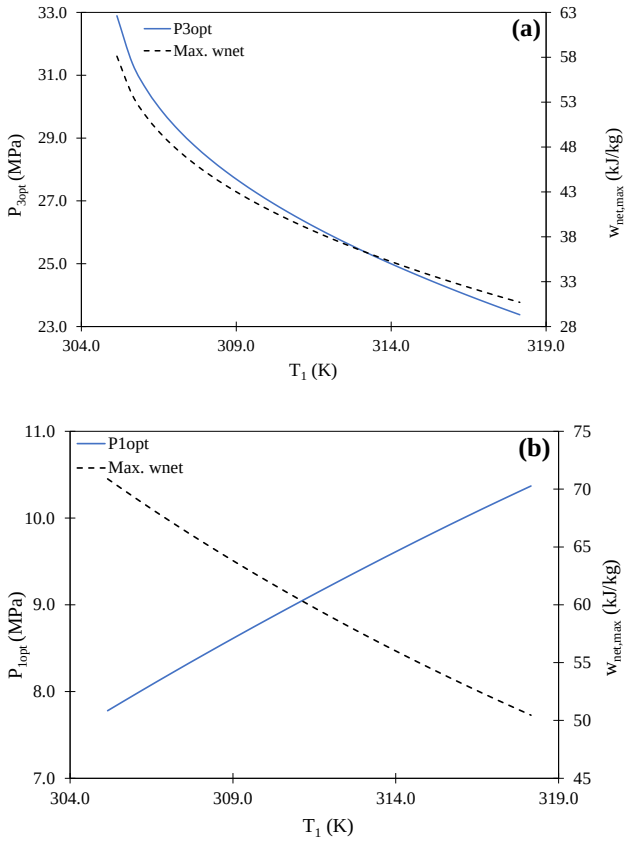

Fig. 7. Effect of compressor inlet temperature on (a) P_{3opt} and $w_{net,max}$ (b) P_{1opt} and $w_{net,max}$.

Figures 8(a) and 8(b) present the effects of turbine inlet temperature T_3 on the optimum compressor inlet pressure and the optimum turbine inlet pressures, respectively. The figures also describe the change of maximum net specific work when the turbine inlet temperature changes. From Figure 8(a), as T_3 increases, the turbine inlet pressure can shift up to gain more net specific work. Therefore, increase in T_3 causes increasing P_{3opt}. As P_{3opt} increases, the compressor and turbine specific works increase. However, when T_3 raises, the turbine specific work grows with higher increasing rate than that of compressor specific work. Therefore, $w_{net,max}$ increases. For fixed P_3, increasing T_3 leads to reducing P_{1opt} and increasing $w_{net,max}$, as shown in Figure 8(b). This is because the increased energy input at the turbine allows the compressor to operate at a slightly lower inlet pressure while still maintaining a high net specific work. Based on Figure 8(a), increase of T_3 has positive effect on $w_{net,max}$. However, at higher T_3 , such as 773.15K, if P_1 is fixed at 7.5 MPa, P_{3opt} is 40.46 MPa and $w_{net,max}$ is 77.51 kJ/kg. It should be observed that this value of P_{3opt} (40.46 MPa) may be beyond heat exchanger application limit. Nevertheless, the result from the second model shown in Figure8(b) indicates that for P_3 at 30.0 MPa, operation of regenerative sCO_2 Brayton cycle with T_3= 773.15K can achieve $w_{net,max}$ of 92.91 kJ/kg using P_{1opt} of 8.34 MPa. This operation condition seems better than the first operation condition and this is the useful of the second model developed in this study.

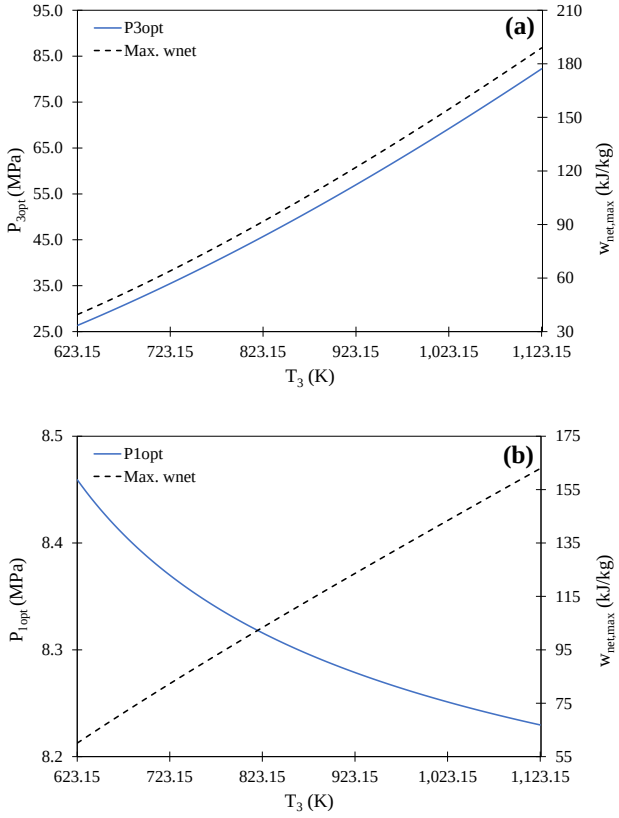

Fig. 8. Effect of turbine inlet temperature on (a) P_{3opt} and $w_{net,max}$ (b) P_{1opt} and $w_{net,max}$.

4.4 Effects of Compressor and Turbine Efficiencies

Figures 9(a) and 9(b) present the effects of compressor and turbine efficiencies, respectively, on the optimum turbine inlet pressure as well as the maximum net specific work. From figures, P_{3opt} increases as η_C or η_T increases. The optimum operating point shifts from P_{3opt} = 28.33 MPa to P_{3opt} = 37.12 MPa, when η_C increases from 0.75 to 0.95 while increase of η_T from 0.75 to 0.95 causes increase in P_{3opt} by 8.1 MPa. The effect of increasing η_C or η_T on P_{3opt} is due to the fact that when η_C increases, the required specific compressor work decreases, causing P_{3opt} to shift to a higher value in order to obtain more net specific work. Similarly,

when η_T increases, more specific turbine work can be produced, potentially leading to an increase in P_{3opt} to achieve greater net specific work. For $w_{net,max}$, as expected, the increase inη_C or η_T introduces increasing $w_{net,max}$. However, comparison between $w_{net,max}$ shown in Figures 9(a) and 9(b), presents that $w_{net,max}$ can be enhanced by increasing η_T more than that by increasing η_C.

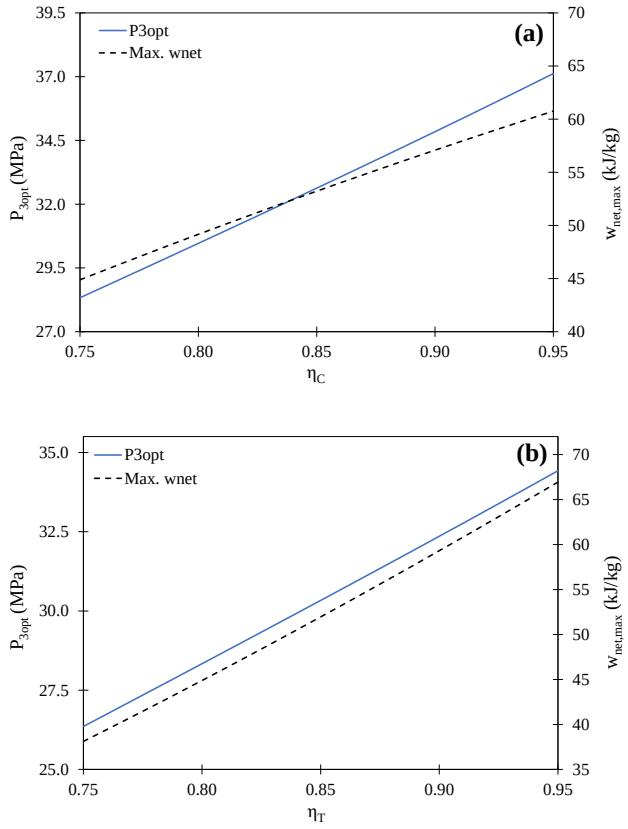

Fig. 9. Effects of (a) η_C and (b) η_T on P_{3opt} and $w_{net,max}$.

For the effects of η_C and η_T on the optimum compressor inlet pressure and the maximum net specific work, these are described in Figures 10(a) and 10(b). From the figures, the change in η_C and η_T from 0.75 to 0.9 reduce, respectively, 0.11 and 0.12 MPa of P_{1opt} It can be said that changing one of the efficiencies slightly affect the value of P_{1opt}. The figures also clearly indicate that increase in η_C or η_T has positive effect on $w_{net,max}$ and increasing η_T can boost $w_{net,max}$ better than increasing η_C can do. Based on the operating parameters defined in Table 3, increase in η_T from 0.75 to 0.95 can increase 47.7% of $w_{net,max}$ while increase in η_C from 0.75 to 0.95 can increase 14.9% of $w_{net,max}$.

This study primarily focuses on identifying the optimum turbine and compressor inlet pressures to maximize the net specific work of a regenerative sCO_2 Brayton cycle. However, there are several practical challenges and limitations that should be considered in future research. Firstly, the high operating pressures, especially at the turbine inlet, may exceed the structural limits of commercial heat exchangers, posing risks related to material strength, fatigue, and cost. Secondly, pressure drops and non-idealities in actual systems, such as heat exchangers, can significantly deviate from the idealized models presented here. Future studies could explore the integration of this model with detailed component-level simulations and experimental validation to account for such practical constraints.

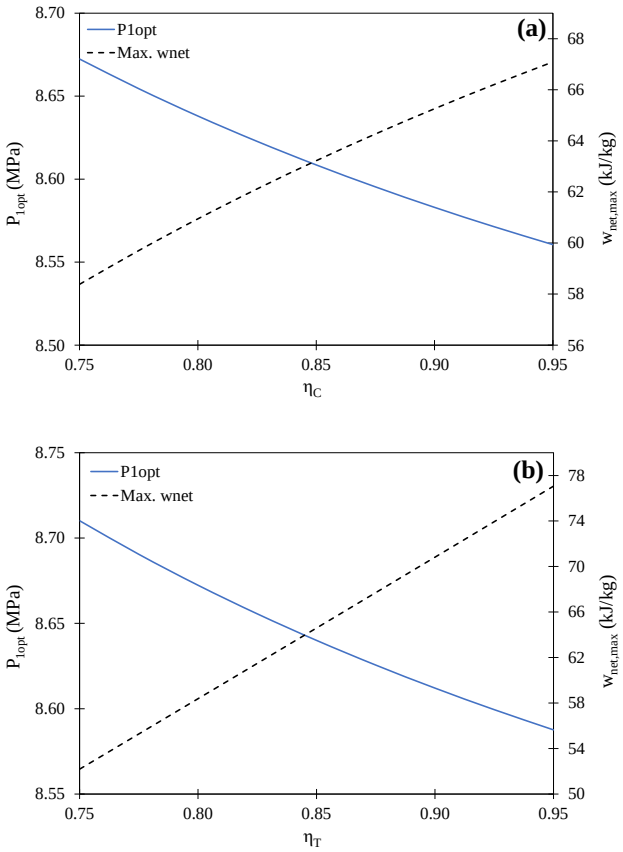

Fig. 10. Effects of (a) η_C and (b) η_T on P_{1opt} and $w_{net,max}$.

5. CONCLUSION

In this study, the relations for finding the optimum turbine and compressor inlet pressures, maximizing net specific work obtained from the regenerative sCO_2 Brayton cycle, were found. These relations were developed based on the real gas CO_2 properties. The effects of operating parameters on the optimum pressures and maximum net specific work were also studied. The main conclusions drawn from the study are summarized as follows:

- The developed formulas, based on real gas properties and expressed in dimensionless form, offer significantly greater accuracy than traditional ideal gas models, particularly in the supercritical region where CO_2 exhibits highly non-linear behavior. The proposed formulation provides more reliable and realistic predictions for high-pressure range.
- Within the defined ranges of operating parameters, the optimum turbine inlet pressure, maximizing net specific work, can be found under varying operational conditions. In contrast, the optimal compressor inlet pressure, associated with the peak of net specific work, may not be found under certain circumstances, particularly at low turbine

inlet pressure and elevated turbine and/or compressor inlet temperatures.

- An increase in the compressor inlet pressure leads to an increase in the optimum turbine inlet pressure and thus to an increase in the maximum specific net work. An increase in the turbine inlet pressure leads to a slight increase in the optimum compressor inlet pressure. The specific net work then increases.
- The optimum turbine inlet pressure P_{3opt} corresponding to the compressor inlet pressure P_1 and the optimum compressor inlet pressure P_{1opt} corresponding to the turbine inlet pressure P_3 do not constitute identical pairs, underscoring the intricate interplay of these parameters.
- Elevated compressor inlet temperature results in a reduction of the optimal turbine inlet pressure and an increase in the optimal compressor inlet pressure, leading to a reduction in the maximum net specific work. Conversely, increasing turbine inlet temperature causes effects opposite to those observed with increasing compressor inlet temperature.
- Improvements in turbine and compressor efficiencies exert a positive influence by causing an increase in the optimal turbine inlet pressure and a reduction in the optimal compressor inlet pressure, thereby enhancing the maximum net specific work.
- The parametric analysis indicated that compressor and turbine inlet temperatures, isentropic efficiencies, and pressure conditions affect the optimum points. There is no single combination that fits the tailored design based on application-specific constraints.

6. FUTURE SCOPE AND RECOMMENDATIONS

This study provides theoretical relations for determining the optimum compressor and turbine inlet pressures in a regenerative sCO_2 Brayton cycle using real gas properties. To improve the applicability of the proposed model, some topics can be explored in future research. These include:

- Incorporating pressure drops in all major components to reflect realistic operation conditions.
- Investigating the performance of heat exchangers affected the cycle power output.
- Assessing the feasibility of the system with respect to material limitations, operational safety, and cost considerations in real applications.

NOMENCLATURE

ARD	=	absolute relative difference (%)
f_1	=	function defined by Equation 6
f_2	=	function defined by Equation 11
h	=	specific enthalpy (kJ/kg)
k	=	ideal gas specific heat ratio
P	=	pressure (kPa)
ΔP	=	pressure drop (kPa)
s	=	specific entropy (kJ/kg·K)
sCO_2	=	supercritical carbon dioxide
T	=	temperature (K)
ΔTT	=	terminal temperature difference (K)
v	=	specific volume (m^3/kg)
w	=	specific work (kJ/kg)

Greek symbols

β	=	thermal expansion coefficient (K^{-1})
η	=	isentropic efficiency
ρ	=	density (kg/m^3)

Subscript

C	=	compressor
IG	=	ideal gas
max	=	maximum value
net	=	net value
opt	=	optimum value
s	=	isentropic process
T	=	turbine
1, 2	=	compressor inlet and outlet states
3, 4	=	turbine inlet and outlet states

REFERENCES

[1] Zhang X., Yu L., Li M., and Song P., 2020. Simulation of a supercritical CO_2 recompression cycle with zero emissions. *Journal of Energy Engineering* 146(6): 04020059. https://doi.org/10.1061/(ASCE)EY.1943-7897.0000711.

[2] Wang K., He Y.L., and Zhu H.H., 2017. Integration between supercritical CO_2 Brayton cycles and molten salt solar power towers: a review and a comprehensive comparison of different cycle layouts. *Applied Energy* 195 (Jun): 819-836. https://doi.org/10.1016/j.apenergy.2017.03.099

[3] Wu P., Ma Y., Gao C., Liu W., Shan J., Huang Y., Wang J., Zhang D., and Ran X.. 2020. A review of research and development of supercritical carbon dioxide Brayton cycle technology in nuclear engineering applications. *Nuclear Engineering and Design* 368 (Nov): 110767.

[4] Luo D. and D. Huang. 2020. Thermodynamic and exergoeconomic investigation of various sCO2 Brayton cycles for next generation nuclear reactors. *Energy Conversion and Management* 209 (Apr): 112649.

[5] Atif M. and F.A. Al-Sulaiman. 2018. Energy and exergy analyses of recompression Brayton cycles integrated with a solar power tower through a two-tank thermal storage system. *Journal of Energy*

Engineering 144(4):04018036. https://doi.org/10.1061/(ASCE)EY.1943-7897.0000545.

[6] Wang X., Liu Q., Bai Z., Lei J., and Jin H., 2018. Thermodynamic investigations of the supercritical CO2 system with solar energy and biomass. *Applied Energy* 227 (Oct): 108-118. https://doi.org/10.1016/j.apenergy.2017.08.001

[7] Gan Q., Candela T., Wassing B., Wasch L., Liu J., and Elsworth D., 2012. The use of supercritical CO_2 in deep geothermal reservoirs as a working fluid: Insights from coupled THMC modeling. *International Journal of Rock Mechanics and Mining Sciences* 147(Nov): 104872. https://doi.org/10.1016/j.ijrmms.2021.104872.

[8] Feher E.G., 1968. The supercritical thermodynamic power cycle. *Energy Conversion* 8(2): 85-90. https://doi.org/10.1016/0013-7480(68)90105-8

[9] Dostal V., 2004. A supercritical carbon dioxide cycle for next generation nuclear reactors. *Ph.D. dissertation*, Department of Nuclear Engineering, MIT., Cambridge, MA, USA.

[10] Zhang C., Yan L., and Shi J., 2023. Performance prediction of a supercritical CO_2 Brayton cycle integrated with wind farm-based molten salt energy storage: Artificial intelligence (AI) approach. *Case Studies in Thermal Engineering* 51 (Nov): 103533, https://doi.org/10.1016/j.csite.2023.103533.

[11] Haseli Y., 2013. Optimization of a regenerative Brayton cycle by maximization of a newly defined second law efficiency. *Energy Conversion and Management* 68 (Apr): 133-140. https://doi.org/10.1016/j.enconman.2012.12.033

[12] Vélez F., Segovia J., Chejne F., Antolín G., Quijano A., and Martín M.C., 2011. Low temperature heat source for power generation: Exhaustive analysis of a carbon dioxide transcritical power cycle. *Energy* 36(9): 5497-5507. https://doi.org/10.1016/j.energy.2011.07.027.

[13] Song Y., Wang J., Dai Y., and Zhou E., 2012. Thermodynamic analysis of a transcritical CO_2 power cycle driven by solar energy with liquified natural gas as its heat sink. *Applied Energy* 92 (Apr): 194-203. https://doi.org/10.1016/j.apenergy.2011.10.021.

[14] Mondal S. and De S., 2015. CO_2 based power cycle with multi-stage compression and intercooling for low temperature waste heat recovery. *Energy.* 90 (Oct): 1132-1143. https://doi.org/10.1016/j.energy.2015.06.060.

[15] Memon A.G., Harijan K., Uqaili M.A., and Memon R.A., 2013. Thermo-environmental and economic analysis of simple and regenerative gas turbine cycles with regression modeling and optimization. *Energy Conversion and Management* 76 (Dec): 852-864. https://doi.org/10.1016/j.enconman.2013.07.076.

[16] Javanshir A., Sarunac N., and Razzaghpanah Z., 2018. Thermodynamic analysis of simple and regenerative Brayton cycles for the concentrated solar power applications. *Energy Conversion and Management* 163 (May): 428-443. https://doi.org/10.1016/j.enconman.2018.02.079

[17] Ehsan M.M., Guan Z., Klimenko A.Y., and Wang X., 2018. Design and comparison of direct and indirect cooling system for 25 MW solar power plant operated with supercritical CO2 cycle. *Energy Conversion and Management* 168: 611-628. https://doi.org/10.1016/j.enconman.2018.04.072.

[18] Ehsan M.M., Duniam S., Li J., Guan Z., Gurgenci H., and Klimenko A., 2020. A comprehensive thermal assessment of dry cooled supercritical CO_2 power cycles. *Applied Thermal Engineering*, 166: 114645. https://doi.org/10.1016/j.applthermaleng.2019.114645

[19] Khadse A., Blanchette L., Kapat J., Vasu S., Hossain J., and Donazzolo A., 2018. Optimization of supercritical CO_2 Brayton cycle for simple cycle gas turbines exhaust heat recovery using genetic algorithm. *Journal of Energy Resources Technology* 140(7): 071601. https://doi.org/10.1115/1.4039446.

[20] Ruiz-Casanova E., Rubio-Maya C., Pacheco-Ibarra J.J., Ambriz-Díaz V.M., Romero C.E., and Wang X., 2020. Thermodynamic analysis and optimization of supercritical carbon dioxide Brayton cycles for use with low-grade geothermal heat sources. *Energy Conversion and Management* 216 (Jul): 112978. https://doi.org/10.1016/j.enconman.2020.112978.

[21] Wang X., Wang J., Zhao P., and Dai Y., 2016. Thermodynamic comparison and optimization of supercritical CO_2 Brayton cycles with a bottoming transcritical CO_2 cycle. *Journal of Energy Engineering* 142(3): 04015028. https://doi.org/10.1061/(ASCE)EY.1943-7897.0000292.

[22] Rao Z., Xue T., Huang K., and Liao S., 2019. Multi-objective optimization of supercritical carbon dioxide recompression Brayton cycle considering printed circuit recuperator design. *Energy Conversion and Management* 201(Dec): 112094. https://doi.org/10.1016/j.enconman.2019.112094.

[23] Jin Q., Xia S., Li P., and Xie T., 2022. Multi-objective performance optimization of regenerative S-CO_2 Brayton cycle based on neural network prediction. *Energy Conversion Management X.* 14(May): 100203. https://doi.org/10.1016/j.ecmx.2022.100203.

[24] Oyewola O.M., Petinrin M.O., Labiran M.J., and Bello-Ochende T., 2023. Thermodynamic optimisation of solar thermal Brayton cycle models and heat exchangers using particle swarm algorithm. *Ain Shams Engineering Journal* 14(4): 101951. https://doi.org/10.1016/j.asej.2022.101951.

[25] Moran M.J., Shapiro H.N., Boetter D.D., and Bailey M.B., 2014. *Fundamentals of Engineering Thermodynamics*. US.: Wiley.

[26] Gülen S.C., 2019. *Gas Turbine Combined Cycle Power Plants*. US.: CRC Press.

[27] Jarungthammachote S., 2022. Optimal interstage pressures of multistage compression with intercooling processes. *Thermal Science and*

Engineering Progress 29 (Mar): 101202. https://doi.org/10.1016/j.tsep.2022.101202.

[28] Marchionni M., Bianchi G., and Tassou S.A., 2020. Review of supercritical carbon dioxide (sCO_2) technologies for high-grade waste heat to power conversion. *SN Applied Sciences* 2(Mar): 611. https://doi.org/10.1007/s42452-020-2116-6.

[29] White M.T., Bianchi G., Chai L., Tassou S.A., and Sayma A.I., 2021. Review of supercritical CO_2 technologies and systems for power generation. *Applied Thermal Engineering* 185 (Feb): 116447. https://doi.org/10.1016/j.applthermaleng.2020.116447.

[30] Gad-Briggs A., and P. Pilidis. 2017. Analyses of simple and intercooled recuperated direct Brayton helium gas turbine cycles for generation IV reactor power plants. *ASME Journal of Nuclear Engineering and Radiation Science* 3(1): 011017. https://doi.org/10.1115/1.4033398.

[31] Span R., and W.A. Wagner. 1996. New equation of state for carbon dioxide covering the fluid region from the triple-point temperature to 1100 K at pressures up to 800 MPa. *Journal of Physical and Chemical Reference Data* 25(6): 1509-1596.https://doi.org/10.1063/1.555991.

[32] McBride B.J., Zehe M.J., and Gordon S., 2002. NASA Glenn Coefficients for Calculating Thermodynamic Properties of Individual Species. Cleveland, Ohio: NASA.

[33] Lemmon E.W., Bell I.H., Huber M.L., and McLinden M.O., 2023. Thermophysical Properties of Fluid Systems. Accessed July 29, 2023. https://webbook.nist.gov/chemistry/fluid.

[34] Hossain M.J., Chowdhury J.I., Balta-Ozkan N., Asfand F., Saadon S., and Imran M., 2021. Design optimization of supercritical carbon dioxide (s-CO_2) cycles for waste heat recovery from marine engines. *ASME Journal of Energy Resources Technology* 143(12): 120901. https://doi.org/10.1115/1.4050006.